Decoding the dynamic of poleward shifting climate zones using aqua-planet model simulation

Hu Yang (hu.yang@awi.de)
Alfred-Wegener-Institut Helmholtz-Zentrum fur Polar- und Meeresforschung https://orcid.org/0000-0003-2054-2256

Jian Lu
PNNL: Pacific Northwest National Laboratory

Xiaoxu Shi
AWI: Alfred-Wegener-Institut Helmholtz-Zentrum fur Polar- und Meeresforschung

Qiang Wang
AWI: Alfred-Wegener-Institut Helmholtz-Zentrum fur Polar- und Meeresforschung

Gerrit Lohmann
AWI: Alfred-Wegener-Institut Helmholtz-Zentrum fur Polar- und Meeresforschung

Research Article

Keywords: Tropical expansion, Poleward shift, Ocean circulation, Atmosphere circulation, climate zones

Posted Date: March 17th, 2021

DOI: https://doi.org/10.21203/rs.3.rs-334740/v1

Version of Record: A version of this preprint was published at Climate Dynamics on January 5th, 2022.
See the published version at https://doi.org/10.1007/s00382-021-06112-0.

Climate Dynamics manuscript No.
(will be inserted by the editor)

Decoding the dynamic of poleward shifting climate zones using aqua-planet model simulations

Hu Yang · Jian Lu · Xiaoxu Shi · Qiang Wang · Gerrit Lohmann

Received: date / Accepted: date

Hu Yang · Xiaoxu Shi · Qiang Wang · Gerrit Lohmann
Alfred Wegener Institute, Helmholtz Centre for Polar and Marine Research, Bremerhaven, Germany
Tel.: +49-471-48311897
E-mail: hu.yang@awi.de

Jian Lu
Atmospheric Sciences and Global Change Division, Pacific Northwest National Laboratory, Richland, Washington, USA

Abstract Growing evidence implies that the atmospheric and oceanic circulation experiences a systematic poleward shift in a warming climate. However, the complexity of climate system, including the coupling between the ocean and the atmosphere, natural climate variability and land-sea distribution, tends to obfuscate the causal mechanism underlying the circulation shift. Here, using an idealized coupled aqua-planet model, we explore the mechanism of the shifting circulation, by isolating the contributing factors from the direct CO_2 forcing, the indirect ocean surface warming, and the wind-stress feedback from the ocean dynamics. We find that, in contrast to direct CO_2 forcing, an enhanced subtropical ocean warming plays a leading role in driving the circulation shift. This enhanced subtropical ocean warming emerges from the background Ekman convergence of surface anomalous heat in the absence of the ocean dynamical change. It expands the tropical warm water zone, causes a poleward shift of the meridional temperature gradients, hence forces a corresponding shift in the atmospheric circulation. The shift in the atmospheric circulation in turn drives a shift in the ocean circulation. Our simulations, despite being idealized, capture the main features of observed climate changes, for example, the enhanced subtropical ocean warming, poleward shift of the patterns of near-surface wind, sea level pressure, storm tracks, precipitation and large-scale ocean circulation, implying that increase in greenhouse gas concentrations not only raises the temperature, but can also systematically shift the climate zones poleward.

Keywords Tropical expansion · Poleward shift · Ocean circulation · Atmosphere circulation · climate zones

1 Introduction

An increasing amount of evidence suggests that the atmospheric and oceanic circulation is shifting towards the poles under climate change (Fu et al, 2006; Hu and Fu, 2007; Lu et al, 2007; Seidel et al, 2008). For example, poleward migration of the patterns of storm tracks (Yin, 2005), winds (Chen et al, 2008), jet

streams (Archer and Caldeira, 2008), precipitation (Scheff and Frierson, 2012), tropical cyclones (Kossin et al, 2014), cloud (Norris et al, 2016) and large-scale ocean circulation (Yang et al, 2016b, 2020a) have been documented based on various observations and climate simulations. These changes redistribute the natural resources, such as water, vegetation and marine primary productivity, thus having broad implications for our societies (Heffernan, 2016). Understanding the underlying causes of the shifting circulation does not only help us to understand why it happens, but also serve to better predict and boost our confidence in the global warming induced changes.

In the past decades, numerous investigations have been carried out to decode the mechanisms (Staten et al, 2018; Shaw, 2019). Early studies have been mainly focused on the atmospheric processes in driving the shift in the atmospheric circulation, concentrating on a specific topic named tropical expansion (Fu et al, 2006; Seidel et al, 2008; Chen et al, 2008). Without involving changes in the ocean, climate model simulations can reproduce the tropical expansion by changing the atmospheric concentration of greenhouse gases (Lu et al, 2007), ozone (Thompson et al, 2011; Polvani et al, 2011), aerosols (Allen et al, 2012) or by introducing uniform sea surface temperature (SST) warming (Chen et al, 2013). However, observations imply that the spatiotemporal variations of SST play a dominant role in driving the recent tropical expansion (Allen and Kovilakam, 2017; Grise et al, 2019). And those SST variations were interpreted as a feature of fluctuations of the Pacific Decadal Oscillation, which is one of the internal climate variabilities. Therefore, growing number of studies suggest that the observed tropical expansion is more attributable to the natural climate variability than the anthropogenic climate change. More recently, following the discovery of shifting large-scale ocean circulation, Yang et al (2020a,b) highlighted that the entire atmospheric and oceanic circulation is moving towards the poles, which is not solely owing to natural climate variability. This is because that many of the observed climate trends, such as the patterns of sea level pressure (SLP), sea surface height (SSH) and near-

surface winds, resemble well with the patterns obtained from the climate simulations forced by increasing greenhouse gases. Yang et al (2020b) proposed that an enhanced subtropical ocean warming (Fig. 1) with an oceanic origin contributes to a poleward advancing of the meridional temperature gradient (MTG), driving the circulation shift.

Due to the coupled nature between the atmosphere and ocean, it is challenging to tease out the causality for the shift of the circulation. For example, it is still not well known whether the shift in the atmosphere circulation drives the shift in the ocean circulation, or vice versa. Could the forced climate change generate an enhanced subtropical ocean warming, or it only emerges temporarily due to natural climate oscillation? To provide insight on these questions, we consider a simplified ocean-atmosphere coupled aquaplanet framework, without asymmetric land-sea distribution, sea ice and deep ocean circulation. Within the framework, we manipulate the configurations of the forcing so as to isolate the impacts of the direct radiative forcing from increasing CO_2 and the indirect one through SST warming. Additionally, by specifying the wind stress seen by the ocean, we further isolate the circulation response without the wind-stress feedback from the ocean adjustment. This idealized approach allows us to partition the full circulation response into different mechanisms in a quantitative manner, so as to poinpoint the leading cause for the circulation shifts in both ocean and atmosphere.

2 Experiments and Methodology

2.1 Experiment design

We used a coupled aqua-planet setup of the Alfred Wegener Institute Earth System Model (AWI-ESM, Sidorenko et al (2015); Rackow et al (2018)), in which the Earth is mostly covered by ocean, except the region higher than 85 degrees (Fig. S1). The atmospheric component is ECHAM6 (Stevens et al, 2013) with a horizontal resolution of 3.75 degrees (T31 grid). The coupled ocean component is FESOM1.4

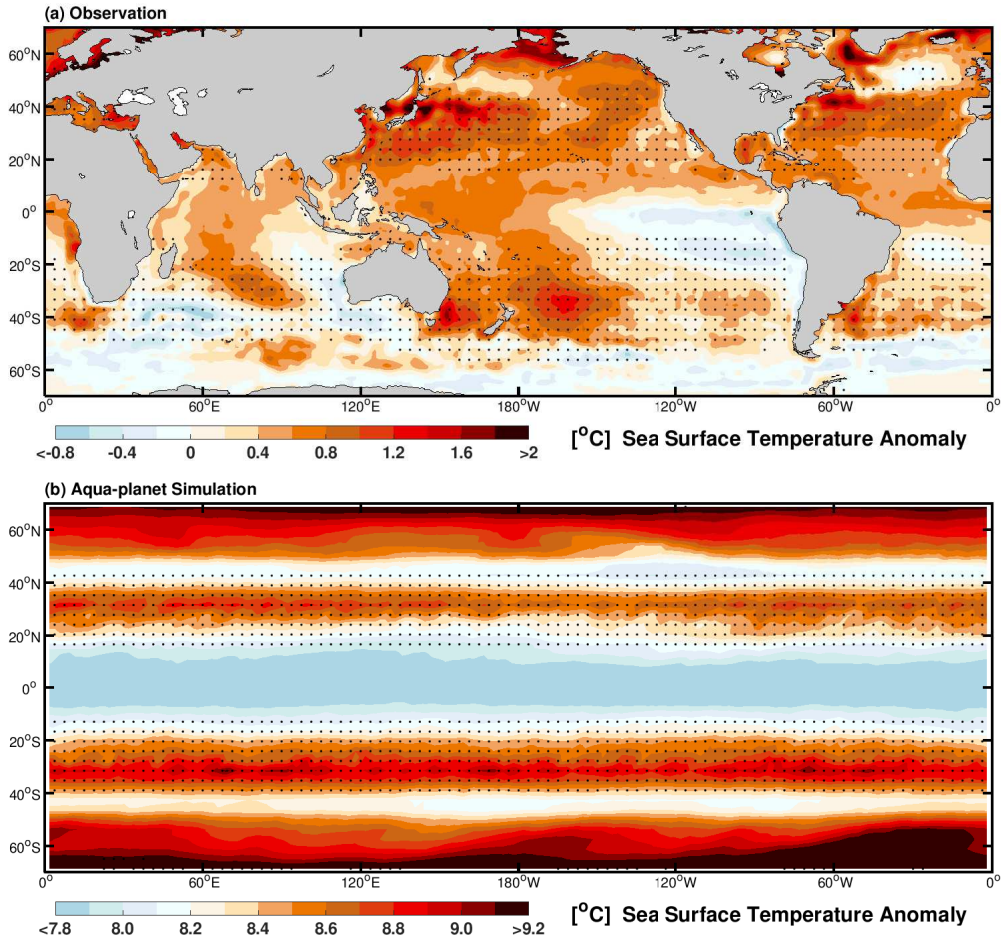

Fig. 1 a: Observational Sea Surface Temperature (SST) anomaly during the most recent five years of satellite period (2016-2020) with respect to the first five years (1982-1986). Relatively stronger ocean surface warming is found over all the subtropical oceans, likely due to the Ekman convergence of background surface ocean currents. Result based on the NOAA Optimum Interpolation (OI) SST V2 dataset. The stippled area shows the subtropical convergence zone based on the near-surface wind stress curl fields from the NCEP-DOE reanalysis (1982-2020). b: Similar to A, but for SST anomaly in the last 40 years of the aqua-planet C1 global warming experiment with respect to the C0 control experiment. Unlike the zonally symmetric enhanced subtropical ocean warming in the aqua-planet simulation, the observational enhanced subtropical ocean warming concentrates more towards the western ocean basins, where the centres of the subtropical gyres locate.

(Wang et al, 2014) with a resolution of approximately 2.5 degrees. The atmosphere has 47 vertical layers, and the ocean has 7 layers and a uniform shallow water depth of 100 m. The shallow ocean setup can well mimics the main structure of

the wind-driven ocean circulation (Fig. 2). The coupling time step is set to be one hour.

We preform two simulations using the fully coupled AWI-ESM, i.e., a control experiment (i.e., C0) and a global warming experiment (i.e., C1). The control simulation (C0) is integrated for 640 years under the pre-industrial CO_2 level (i.e., 284 ppmv). The global warming simulation (C1) is initialized from the 500th model year of the C0 experiment and integrated for 140 years by increasing the concentration of CO_2 linearly from 284 ppmv to 1284 ppmv within 100 years. Afterwards, the CO_2 level is kept constant at the value of 1284 ppmv (Fig. 3). The hourly coupling fields of SST and near-surface wind stress from the C0 and C1 experiments are saved and used later in the partially coupled simulations.

To quantify the contribution of CO_2 and SST in driving the atmospheric circulation shift, we perform two partially coupled experiments, i.e., C1T0 and C0T1. In the C1T0 experiment, we increase the CO_2 as in the C1 global warming experiment, but replace the hourly coupling SST field in the atmosphere model with that from the control experiment (i.e., C0). Different from the C1T0 experiment, the C0T1 experiment is integrated with the constant pre-industrial CO_2 level, but the SST is replaced with that from the global warming experiment (i.e., C1).

To explore the dynamic of the systematic shift in circulation, we carry out another three partially coupled simulations, i.e., C1W0, C0W1 and C0W0. In the C1W0 experiment, we increase the CO_2 as in the C1 global warming experiment, but the hourly coupling near-surface wind stress into the ocean model is replaced with that from the C0 control experiment. In contrast, the C0W1 experiment is integrated under constant pre-industrial CO_2 level, but replace the winds with that from the C1 global warming experiment, which contains a signal of poleward shift. As replacing wind stress itself could introduce climate anomaly, we perform the third experiment, i.e., C0W0, as a reference control run for the partially coupled simulations. It runs under constant pre-industrial CO_2 level, with the wind taken from the C0 experiment. The 499th model year of the C0 experiment is used to

initialize all these partially coupled experiments. Note that if the 500th model year of C0 experiment is used to initialize, the C0W0 result will be identical to that of the C0 experiment. The last 40 years of the sensitivity experiments (i.e., C1, C1T0, C0T1, C0W1, C1W0) are used to compare with the 140 years of the control experiments (i.e., C0 and C0W0). Table 1 summaries the above mentioned experiments.

Table 1 List of aqua-planet simulations in this study.

Experiment Name	Initial Condition	Simulation Years	Brief Description
C0	Prescribed zonally constant climate fields	640	Pre-industrial control run, constant CO_2 level at 284 ppmv.
C1.	500th year of the C0 experiment	140	Global warming run, linearly increase the CO_2 from 284 ppmv to 1284 ppmv within 100 years, keep it constant at 1284 ppmv level afterwards
C1T0	500th year of the C0 experiment	140	Increase CO_2 as in C1, but replace the coupling SST from C0
C0T1	500th year of the C0 experiment	140	Keep CO_2 constant as in C0, but replace the coupling SST from C1
C0W0	499th year of the C0 experiment	140	Partially coupled control run, keep CO_2 constant as in C0, but replace the coupling winds from C0
C0W1	499th year of the C0 experiment	140	Keep CO_2 constant as in C0, but replace the coupling winds from C1
C1W0	499th year of the C0 experiment	140	Increase CO_2 as in C1, but replace the coupling winds from C0

2.2 Methodology

We use two metrics to quantify the meridional locations of the atmospheric and oceanic circulation. The location of the atmospheric circulation is obtained as the mean positions of the subtropical high and subpolar low SLP systems over both hemispheres. This is primarily based on the fact that the subtropical high SLP systems locate at the boundary between the Hadley cell and the Ferrel cell, and the subpolar low SLP systems mark the confluence region of the Ferrel cell and

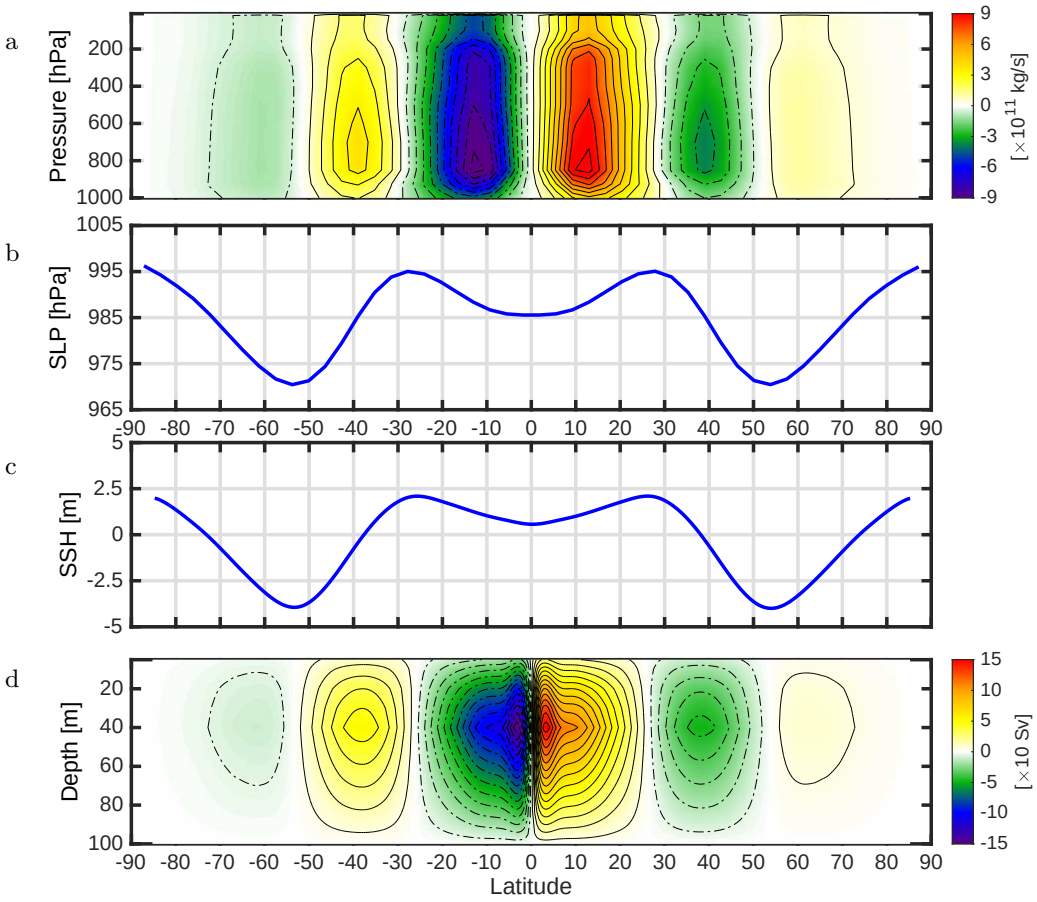

Fig. 2 Climatological patterns of the atmosphere and ocean circulation in the aqua-planet C0 control experiment. a: Stream function of the atmospheric overturning circulation. Positive values represent clockwise flow, and negative values stand for anticlockwise flow. b: Sea level pressure (SLP). Subtropical high SLP is associated with sinking branches of the Hadley cell and the Ferrel cell, while subpolar low SLP is associated with the raising branches of the Ferrel cell and the Polar cell. c: Sea surface height (SSH). Subtropical high SSH represents the centres of the real-world subtropical gyres, while subpolar low SSH denotes the position of the real-world subpolar gyre. d: Stream function of the overturning circulation in the ocean. Positive values represent clockwise flow, and negative values stand for anticlockwise flow.

the Polar cell (Fig. 2). Here, the position of the subtropical high (subpolar low) SLP is defined as the latitude where the zonal mean SLP reaches the peak high (low) value.

Similarly, we track the location of the ocean circulation by calculating the mean meridional positions of the subtropical high and subpolar low SSH, because centers of the subtropical ocean gyres have relative high regional SSH, and the centers of the subpolar gyres are featured by relatively low regional SSH (Yang

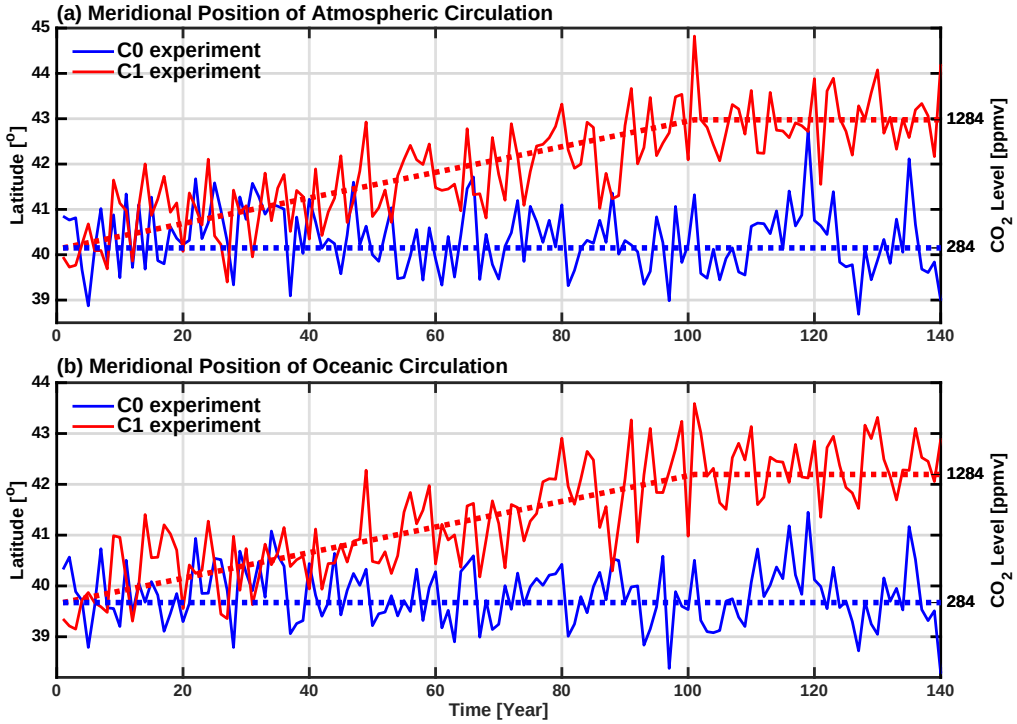

Fig. 3 Meridional position of (a) atmospheric circulation and (b) oceanic circulation in the aqua-planet control (C0, blue lines) and global warming (C1, red lines) experiments. The solid lines represent the meridional position, and the dashed lines are the concentration of CO_2. The displacement of the atmosphere circulation is strongly coupled with that of the ocean circulation. The correlation coefficients between them reach 0.82 and 0.95 in the C0 and C1 experiments, respectively.

et al, 2020a). Here, the position of the subtropical high (or subpolar low) SSH is estimated as the latitude where the zonal mean SSH field peaks.

The anticyclonic winds associated with the subtropical high SLP system drives convergence of surface ocean currents through the Ekman effect (Ekman, 1905), which generates a relatively high regional SSH and a downwelling in the ocean. The opposite case applies for the subpolar low SLP system. Therefore, the SLP pattern in the atmosphere and the SSH pattern in the ocean are intimately dynamically coupled (Fig. 2).

As the modelling framework is statistically zonally symmetric, our analysis focuses only on the zonal mean aspect of the response. To quantify the shifting circulation with better spatial resolution, we interpolate the original zonal mean

data onto a 0.01 degree resolution grid using spline interpolation before our analysis. Finally, it should be noted that our analysis is based on the annual mean result and the seasonality will not be discussed in this paper.

2.3 Observational data

Satellite-derived observational SST (from the NOAA OISST dataset (`https://www.esrl.noaa.gov/psd/`)) and SSH (from the AVISO altimetry (`http://www.aviso.altimetry.fr/duacs/`)) are used to validate our results from the idealized aqua-planet simulations. Besides, the atmospheric reanalysis dataset NCEP-DOE (Kanamitsu et al, 2002) and the ocean reanalysis dataset SODA2.2.0 (Carton and Giese, 2008) are used as well to draw the structure of the atmosphere and ocean circulation in the real world.

3 Results

3.1 Poleward shift of atmospheric and oceanic circulation in a warming climate

Figs. 2 and 4 present the results of the fully coupled aqua-planet model simulations. As shown, the control experiment (C0, blue lines) simulates a SST profile from 33 °C near the equator to 5 °C near the poles. There are easterly near-surface winds at lower latitudes and westerly winds around the mid-latitudes. The precipitation minus evaporation (P-E) pattern illustrates large precipitation at the central tropics (i.e., the Inter Tropical Convergence Zone), and relatively dry subtropics and wet mid-latitudes. The SLP profile shows subtropical high and subpolar low pressure systems, corresponding to the sinking branch of the Hadley cell and rising branch of the Ferrel cell, respectively. Regarding the ocean circulation, relatively high/low SSHs are found near the subtropical/subpolar regions, representing the meridional centres of the subtropical/subpolar ocean gyres in reality. In general, the features generated by our aqua-planet simulation resemble the typical circulation structures shown in the observations (Fig. S2 and S3). It is worth noting

that in our water-planet world, there is no polar sea ice due to a relatively warm ocean near the poles. Previous aqua-planet model simulation also shows the similar feature (Smith et al, 2006), likely owing to strong water exchange between the low and high latitudes maintained by the meridional overturning circulation. The aqua-planet global mean surface temperature (i.e., 21.3 °C) is also higher than that in observation, probably due to the fact that the effective heat capacity in the aqua-planet world is higher than that in the real world (Lohmann, 2019). Since there is no zonal temperature gradient, our aqua-planet world has no fluctuations of El Nino-Southern Oscillation or Pacific Decadal Oscillation.

Comparing with the control run (C0), the global warming experiment (C1) shows a weak polar amplification, even though without sea ice-albedo feedback (Figs. 1b and 4b). Besides, an enhanced ocean warming is identified around the subtropical regions. Such pattern resembles the satellite observed SST anomaly as shown in Fig. 1a. The enhanced subtropical ocean warming induces an anomalous upward ocean surface turbulent heat flux (i.e., sensible+latent heat fluxes, the main form of ocean-atmosphere heat exchange (Yang et al, 2016a)) from the ocean to the atmosphere (Fig. 4d). We notice that the simulated SST anomalies are not hemisphere-symmetric. This is likely due to the asymmetric insolation caused by the Earth's elliptical orbit.

Apart from the changes in SST, under increasing CO_2 forcing, the atmospheric and oceanic circulation experiences a gradually poleward shift of 2.64±0.65° and 2.57±0.55°, respectively (Figs. 3 and 4). Such shift manifests in a systematic poleward migration of the patterns of zonal winds, storm track, P-E, SLP and SSH (red lines in Fig. 4). Yang et al (2020b) proposed that the shift in the atmospheric circulation is primarily due to a poleward shift of the mid-latitude MTGs. Our simulations capture such a feature, with reduced/increased MTG at equator/polar flanks of the maximum mid-latitude MTG zone (Fig. 4a). These simulated shifts resemble the systematic shift in the atmospheric and oceanic circulation as illus-

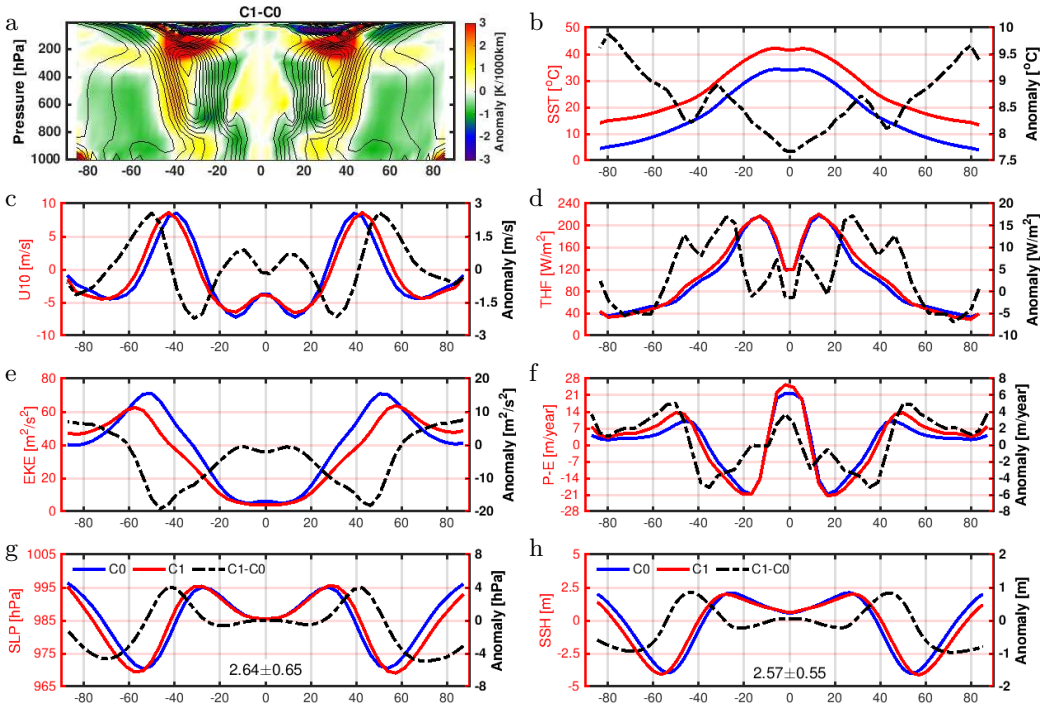

Fig. 4 Comparison between aqua-planet C1 global warming experiment and C0 pre-industrial control experiment. (a). Meridional temperature gradient (MTG) anomaly (shading) in the C1 experiment with respect to the C0 control experiment. The contour lines provide the climatological pattern of the MTG in the C0 experiment. Zonal mean (b) sea surface temperature, (c) zonally near-surface wind, (d) ocean surface turbulent heat flux (THF, i.e., sensible + latent heat fluxes, positive-upward), (e) 850 hPa eddy kinetic energy (EKE) as indication of storm track, (f) precipitation minus evaporation (P-E), (g) sea level pressure (SLP), (h) sea surface height (SSH). The blue lines show the value of the control experiment (C0), the red lines show the values from the global warming experiment (C1), the dashed black lines are the difference between the global warming and the control experiments (C1-C0). The texts in the last two sub-panels provides the magnitudes of the poleward shift in the atmospheric and oceanic circulation, respectively. They are calculated based on the SLP and SSH fields, according to the definition introduced in section 2. All results are based on the last 40 years of the global warming experiment (C1) and 140 years of the control experiment (C0).

trated by various observations and climate simulations (Fu et al, 2006; Chen et al, 2008; Archer and Caldeira, 2008; Scheff and Frierson, 2012; Yang et al, 2020a).

3.2 Dominant role of SST in driving the shift in atmospheric circulation

Compared to the C0 control simulation, the atmosphere circulation shift in the C1 global warming experiment could be driven by two factors, i.e., rising CO_2 concentration and changing SST. In the fully coupled system, the evolutions of

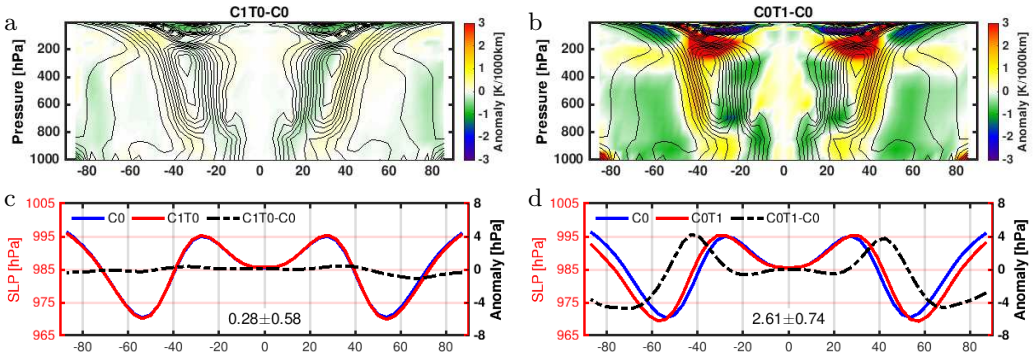

Fig. 5 Similar to Fig. 4, but for comparison between aqua-planet C1T0 (left column, i.e., a and c), C0T1 (right column, i.e., b and d) experiments and the C0 pre-industrial control experiment. (a and b) Meridional temperature gradient (MTG) anomaly (shading). The contour lines provide the climatological pattern of the MTG in the C0 experiment. (c and d) Zonal mean SLP. The blue lines show the value of the control experiment (C0), the red lines show the values from the C1T0 and C0T1 experiment, the dashed black lines are the difference between the two experiments, i.e., C1T0-C0 and C0T1-C0. The poleward shifts in the C1T0 and C0T1 experiments are 0.28 and 2.61 degrees in latitude, respectively. Here, we only show the changes in SLP patterns to indicate the shift in the atmosphere circulation. It should be noted that the other metrics, like the P-E, winds, storm track, have consistent shift as well.

these two factors occur synchronously. Therefore, it is difficult to determine which factor is more important in directly driving the displacement of the atmosphere circulation. To separate these two factors, we design two experiments here, i.e., C1T0 and C0T1 (see Section 2.1).

In the C1T0 experiment, the strong increase in CO_2 induces a 7.6 W/m^2 globally averaged heat imbalanced at the top of atmosphere (not shown). Despite such a strong radiative forcing, the C1T0 experiment shows mild changes in the MTGs and minor shift (0.28±0.58°) in the atmospheric circulation (Fig. 5a and 5c). In contrast, without the CO_2 forcing, the C0T1 experiment (Fig. 5b and 5d) obtains a profound shift in the MTGs, hence, a strong shift (2.61±0.74°) in the atmospheric circulation. Our results indicate that the shift of the atmospheric circulation is primarily driven by the fundamental change in the thermal condition of the underlying ocean, while the direct radiative effect of increasing CO_2 contributes only marginally to the shift of the atmospheric circulation (only around 10 precent in our aqua-planet world).

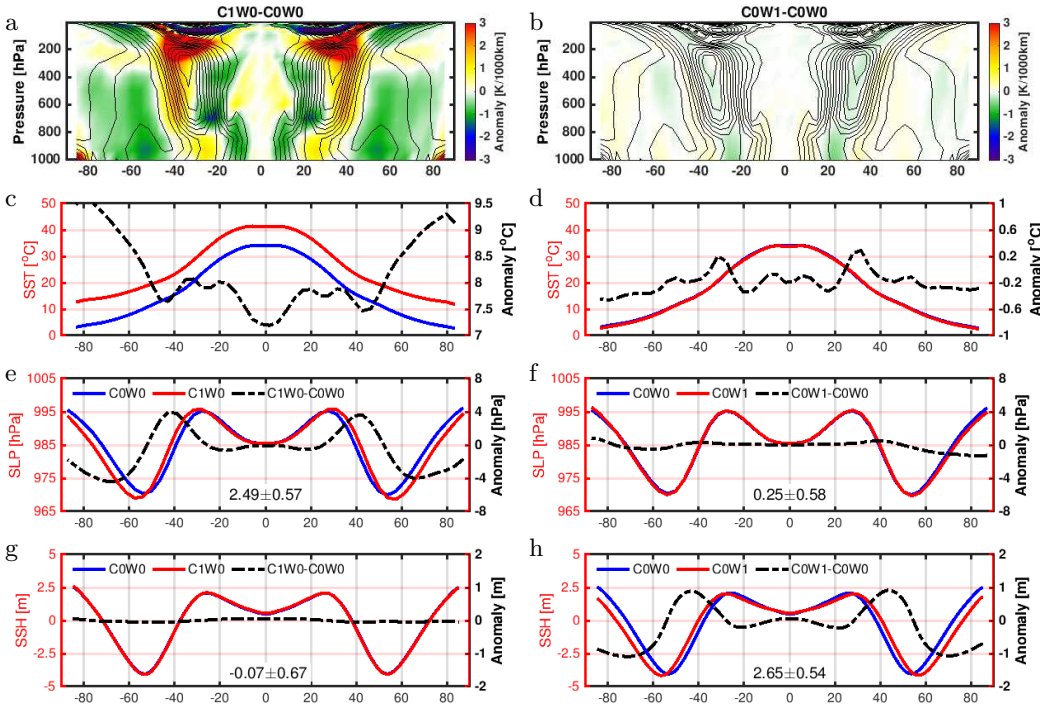

Fig. 6 Similar to Fig. 4, but for results from the partially coupled C1W0 (a, c, e, g) and C0W1 (b, d, f, h) experiments with respect to the C0W0 control experiment.

3.3 Dynamics of shifting atmospheric and oceanic circulation

Previously, Yang et al (2020b) argued that the warming SST pattern, in particularly, the subtropical ocean warming plays a critical role in driving the circulation shift. The subtropical warming works to reduce the MTG over the lower latitudes, and increase it over the higher latitudes, thus promoting a poleward shift in the mid-latitude MTG. The coupled nature between the ocean and the atmosphere obfuscates the origin for the enhanced subtropical ocean warming. To disentangle the causal dynamical processes, we further devise three partially coupled aqua-planet simulations: C1W0, C0W1, and C0W0 (see Section 2.1).

In the first experiment (namely the C1W0), we keep increasing the CO_2 as the global warming experiment (i.e., C1), but using the hourly wind stress fields from the control experiment (i.e., C0) to force the ocean. Note that the wind forcing from the C0 experiment has no signal of shift. As shown in Fig. 6g, the C1W0

experiment does not show a shift in the SSH pattern (-0.07±0.67°), suggesting that the background ocean circulation has no significant change once wind forcing is fixed. Without a change in ocean circulation, we still find a pattern of enhanced subtropical ocean warming (6c). This implies that the enhanced subtropical ocean warming pattern is independent of the ocean circulation change, but generated by the background ocean circulation. Driven by the divergence of surface wind associated with high SLP system, the subtropical ocean is featured by Ekman transport convergence of surface currents (Ekman, 1905). This convergence does not only converge the surface water, but also collects the anomalous heat contained in the water due to climate warming. Therefore, the C1W0 experiment produces a relatively higher SST over the subtropical latitudes. Our result is in agreement with the previous result from a standalone aqua-planet ocean model (Fig. 4d in (Yang et al, 2020b)). Without a shift in the ocean circulation, the C1W0 experiment reproduces a strong shift (2.49±0.57°) in the atmospheric circulation (Fig. 6e), similar to the magnitude of the shift in the C1 experiment (Fig. 4g). This shift is supposed to be driven by the subtropical ocean warming (Fig. **??**c), which pushes the MTG (Fig. 6a) to a higher latitude.

To understand how the ocean circulation responses to a shift in the atmosphere circulation, we show the results from the C0W1 experiment. In this experiment, we keep the CO_2 constant as the C0 control run, but replace the wind field from the C1 global warming experiment, which contains the signal of wind shift (Fig. 4c, red line). As shown in Fig. 6h, under forcing of shifting near-surface winds, the ocean circulation exhibits a significant poleward shift (2.65±0.54°). Combining the results from the C0W1 and C1W0 experiments, we can conclude that rising CO_2 does not directly affect the position of ocean circulation. The displacement of the ocean circulation is primarily driven by the shift in the atmosphere circulation.

Inspecting the C0W1 experiment, we find a minor (around 0.2 °C) SST increase/decrease over the polar/equator flanks of subtropical latitudes (Fig. 6d). This is attributed to the shift in surface ocean circulation, which transports more

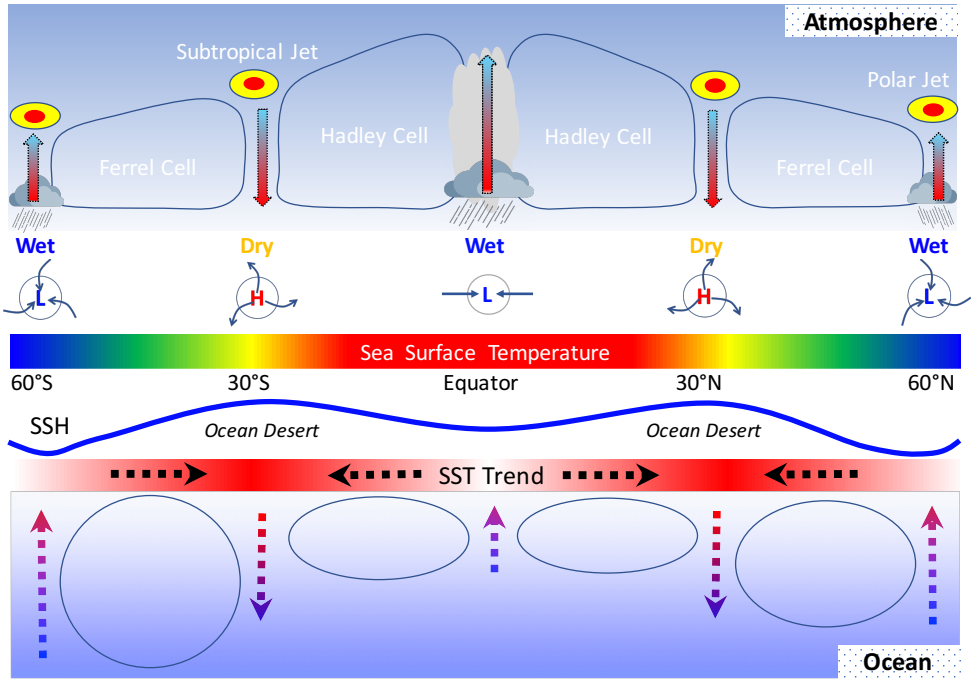

Fig. 7 Schematic diagram showing how background ocean circulation promotes an enhanced subtropical ocean warming and drives the shift in the atmospheric and oceanic circulation. The arrows illustrate the significant features of atmosphere (solid) and ocean (dashed) circulation. From a climatological perspective, the maximum meridional temperature gradients (MTGs) locate at the subtropical to mid-latitude regions. Position of MTGs determines the position of the atmosphere circulation, thus the position of the wind-driven ocean circulation. Under the forcing of increasing greenhouse gases concentration, background Ekman convergence of surface currents favour an enhanced subtropical ocean warming. This enhanced warming expands the low latitude warm water zones, pushes the mid-latitude MTGs towards higher latitudes, thus forcing a poleward shift in the atmosphere circulation. The shift in the atmosphere circulation, associated with a corresponding shift in the near-surface wind then force a shift in the ocean circulation. Systematic shift of atmosphere and ocean circulation redistributes the natural resources, such as water, vegetation, marine primary productivity, hence has broad implications for our societies.

heat from the lower latitudes towards the higher latitudes. In response to such a SST anomaly, the mid-latitude MTG within the troposphere has a slight change (Fig. 6b), contributing to a minor shift ($0.25\pm0.58^{\circ}$) in the atmosphere circulation (Fig. 6f).

In summery, under the CO_2 induced radiative forcing, the background ocean Ekman convergence near the subtropical region generates an enhanced ocean surface warming. This warming causes poleward displacement in the mid-latitude MTG within the troposphere atmosphere, forcing a corresponding shift in the at-

mospheric circulation (Fig. 7). The shift in the atmospheric circulation, manifested with a shift in the near-surface winds, in turn, drives a shift in the ocean circulation. Changes of ocean circulation produce slightly warmer/cooler SST anomalies at the polar/equator flanks of the subtropical ocean, promoting a further minor shift in the atmospheric circulation. Overall, the changes in the ocean thermal condition drive the changes in the atmospheric circulation, which in turn reshapes the wind-driven ocean circulation. Comparably, the feedback from the wind-driven ocean circulation change to the atmospheric circulation is at best secondary.

4 Discussion and conclusions

Despite numerous studies during the past decades, there is still no agreement on the main mechanism driving the tropical expansion and the associated shifting atmospheric and oceanic circulation (Staten et al, 2018; Shaw, 2019; Yang et al, 2020b). Even though climate model simulations can reproduce tropical expansion by including the forcing of CO_2 (Lu et al, 2007), ozone (Thompson et al, 2011; Polvani et al, 2011), or aerosols (Allen et al, 2012), observations show that tropical expansion is primarily related to the variations in SST (Allen and Kovilakam, 2017; Grise et al, 2019). Yang et al (2020b) pointed out that the enhanced subtropical warming plays a central role in driving the shift in the atmospheric circulation .

Following Yang et al (2020b), we use simplified aqua-planet model simulations to demonstrate that, the direct radiative effect of CO_2 is not a potent driver for the shift in the atmosphere circulation. Previously, Staten et al (2012) also drew a similar conclusion by using a more comprehensive atmosphere model. It is the indirect effect of the CO_2 forcing that generates the atmospheric circulation shift through ocean warming, especially that in the subtropics. The enhanced subtropical ocean warming relies on the background ocean circulation, which transports adjacent anomalous ocean heat toward the subtropical regions. This warming contributes to reduce/increase the MTGs over the lower/higher latitudes, therefore driving a shift in the position of the MTG and the atmospheric circulation (Fig.

4). The shift in the atmospheric circulation, in turn, forces a shift in the ocean circulation, helping to further alter the ocean temperature. As a consequence, in a fully coupled system, the enhanced subtropical ocean warming is not centred over the subtropical region, but slightly further shifted toward the polar flank of the mean subtropical gyres (Fig. 1). Our aqua-planet simulations well capture the pattern of subtropical ocean warming, resembling that seen in the observation. Previously, the dynamics of atmospheric circulation changes have also been investigated using other aqua-planet models (Williams and Bryan, 2006; Frierson et al, 2007; Brayshaw et al, 2008; Chen et al, 2010, 2013; Shaw and Tan, 2018). To our knowledge, most of them used only an atmosphere component under prescribed SST forcing. We suggest that the ocean dynamics are important for capturing the full mechanisms of the shifting circulation system.

Poleward shift of the atmosphere circulation has also been reproduced by atmosphere models forced by uniform SST warming (Chen et al, 2013; Grise and Davis, 2020). Such results seem to support the hypothesis that mean warming drives the circulation shift (Frierson et al, 2007; Medeiros et al, 2015; Staten et al, 2014; Son et al, 2018). However, despite spatially uniformed warming, the ocean's heating effect on the atmosphere is not uniform due to the background SST spatial pattern. According to the Stefan-Boltzmann law, increasing 4 K SST from a level of 300 K at lower latitudes could introduce around 6 W/m^2 more upward longwave radiation than that over the higher latitudes (assuming that SST is around 273 K near the sea ice edge, i.e., around 60 degrees). Moreover, previous studies show that warming over the central tropics (Watt-Meyer and Frierson, 2019; Zhou et al, 2019) and polar region (Wu and Smith, 2016; Butler et al, 2010) both contributes to an equatorward contraction of the atmospheric circulation.

By changing the MTG, Yang et al (2020b) reproduced a poleward shift of atmospheric circulation under a global cooling condition. These results hint that mean warming does not necessarily drive a poleward shift of atmosphere circulation. Warming over the central tropics increases the low latitude MTG, leads

to an equatorward contraction of the MTG pattern, and drives an equatorward shift of the atmosphere circulation. By reinforcing the high latitude MTG, cooling, rather than warming over the polar region forces a poleward shift of atmosphere circulation, especially over the high latitudes (Thompson and Solomon, 2002; Min and Son, 2013; Butler et al, 2010). Therefore, we argue that, instead of the mean warming, the shape of the MTG (or the warming pattern), is more important in controlling the location of the atmospheric circulation. We checked the uniform 4 K experiments in the Atmospheric Model Intercomparison Project (Gates et al, 1999). These simulations display a poleward shift of the mid-latitude MTG (not shown) as well, supporting our hypothesis.

The fundamental driver of the atmospheric circulation is the equator-to-pole temperature gradient. From the perspective of climatology, the maximum MTGs are located at the subtropical to mid-latitude regions (Fig. 4a). Their location moves north/south during boreal summer/winter, driving the seasonal displacement of atmospheric and oceanic circulation for more than thousand of kilometers. Therefore, the shape of the equator-to-pole temperature gradients largely controls the position of atmospheric circulation. An enhanced subtropical ocean warming is an efficient way to drive the shift in the mid-latitude MTG, hence, the shift in the atmospheric circulation. Previously, Shaw and Tan (2018) found that introducing CO_2 around the subtropical regions produces the strongest shift in the atmospheric circulation, likely because the CO_2 induces a warming over the subtropical region and thus a poleward shift in the MTG. For the similar reason, model simulations forced by increasing black carbon aerosols and ozone (kind of greenhouse gases) over the mid-latitudes also produce a shift in the atmospheric circulation (Allen et al, 2012). Interestingly, when the shift of atmospheric circulation (or tropical expansion) first drew attention from the scientific community, it was based on the evidence of an enhanced warming over the subtropical troposphere (Fu et al, 2006). This enhanced warming may not only be a manifestation of expanding tropics, but probably also be the reason why the tropics expand. Our study proposes that the

enhanced subtropical warming is not due to atmosphere circulation changes, but has an oceanic origin, which relies on the background oceanic circulation.

The observed enhanced subtropical ocean warming pattern (Fig. 1a) had previously been interpreted as a feature of negative phase of Pacific Decadal Oscillation (Allen and Kovilakam, 2017; Grise et al, 2019). However, Yang et al (2020b) noticed that this warming pattern exists also during periods of positive phase of Pacific Decadal Oscillation, and across all ocean basins. Our aqua-planet simulations, in the absence of fluctuations of Pacific Decadal Oscillation, show that under global warming, background Ekman convergence of subtropical surface current contributes to generating an enhanced subtropical ocean warming, similar to that seen in observation. This hints that, apart from the swing of Pacific Decadal Oscillation, the observed enhanced subtropical ocean warming may also arise from climate change. As the phase of Pacific Decadal Oscillation can flip back and forth, the part of the subtropical warming owing to the increasing greenhouse gases forcing is expect to keep growing in the coming decades, causing a long-standing poleward shift in the atmosphere and ocean circulation.

Last but not least, systematic poleward shift of the circulation has broad manifestations, affecting the atmosphere, ocean, hydrosphere and biosphere. Therefore, the displacement of the large-scale circulation system is plausible to be identified by some regional climate changes. One particular case is the changes of the oceanic western boundary currents, where climate change signal is amplified by the effect of western intensification (Stommel, 1948). Modern long-term observations of the Gulf Stream (Frankignoul et al, 2001) and the Eastern Austrian Current (Ridgway, 2007), show that these currents have undergone a considerable poleward shift in the past more than half a century (Wu et al, 2012; Yang et al, 2016b). This piece of evidence may reflect from a different way that the circulation system has perhaps already moved for a long period. Satellite observations may not capture the full magnitude of the circulation shift due to their short temporal coverages. Paleoclimate proxy records reveal that the Kuroshio Current (Gray et al, 2020), and the

Agulhas Current (Bard and Rickaby, 2009) were several hundred kilometers closer to the equator during the ice age, hinting that the ongoing circulation movement is possible to develop with a great magnitude in the long-term future. Considering that the atmosphere and ocean circulation largely determines the regional climate and the spatial distribution of natural ecosystem, the ongoing shifting circulation is proposed to reshape the climate zones and ultimately cause human migration.

Acknowledgements This work is supported by the AWI INSPIRES program of "Changing Earth - Sustaining our Future". We acknowledge Dirk Barbi for providing the advice on the Message Passing Interface (MPI) coding for the partially coupled aqua-planet model. We would also like to thank the AWI computer centre for supporting the simulation of our study, especially our colleagues Malte Thoma and Natalja Rakowsky. The observational sea surface height data were produced by Ssalto/Duacs and distributed by Aviso, with support from Cnes `http://www.aviso.altimetry.fr/duacs/`. The observational sea surface temperature data (NOAA_OI_SST_V2) is provided by the NOAA/OAR/ESRL PSD, Boulder, Colorado, USA, from their website at `http://https://www.esrl.noaa.gov/psd/` .

Conflict of interest

The authors declare that they have no conflict of interest.

References

Allen RJ, Kovilakam M (2017) The Role of Natural Climate Variability in Recent Tropical Expansion. Journal of Climate 30(16):6329–6350

Allen RJ, Sherwood SC, Norris JR, Zender CS (2012) Recent Northern Hemisphere tropical expansion primarily driven by black carbon and tropospheric ozone. Nature 485(7398):350

Archer CL, Caldeira K (2008) Historical trends in the jet streams. Geophysical Research Letters 35(8)

Bard E, Rickaby RE (2009) Migration of the subtropical front as a modulator of glacial climate. Nature 460(7253):380–383

Brayshaw D, Hoskins B, Blackburn M (2008) The storm-track response to idealized SST perturbations in an aquaplanet GCM. Journal of the Atmospheric Sciences 65(9):2842–2860

Butler AH, Thompson DW, Heikes R (2010) The steady-state atmospheric circulation response to climate change–like thermal forcings in a simple general circulation model. Journal of Climate 23(13):3474–3496

427 Carton JA, Giese BS (2008) A reanalysis of ocean climate using Simple Ocean
428 Data Assimilation (SODA). Monthly Weather Review 136(8):2999–3017
429 Chen G, Lu J, Frierson DM (2008) Phase speed spectra and the latitude of surface
430 westerlies: Interannual variability and global warming trend. Journal of Climate
431 21(22):5942–5959
432 Chen G, Plumb RA, Lu J (2010) Sensitivities of zonal mean atmospheric circu-
433 lation to SST warming in an aqua-planet model. Geophysical Research Letters
434 37(12)
435 Chen G, Lu J, Sun L (2013) Delineating the eddy–zonal flow interaction in the
436 atmospheric circulation response to climate forcing: Uniform sst warming in an
437 idealized aquaplanet model. Journal of the atmospheric sciences 70(7):2214–2233
438 Ekman VW (1905) On the influence of the earth's rotation on ocean-currents.
439 Frankignoul C, de Coëtlogon G, Joyce TM, Dong S (2001) Gulf Stream vari-
440 ability and ocean–atmosphere interactions. Journal of physical Oceanography
441 31(12):3516–3529
442 Frierson DM, Lu J, Chen G (2007) Width of the Hadley cell in simple and com-
443 prehensive general circulation models. Geophysical Research Letters 34(18)
444 Fu Q, Johanson CM, Wallace JM, Reichler T (2006) Enhanced mid-latitude tro-
445 pospheric warming in satellite measurements. Science 312(5777):1179–1179
446 Gates WL, Boyle JS, Covey C, Dease CG, Doutriaux CM, Drach RS, Fiorino M,
447 Gleckler PJ, Hnilo JJ, Marlais SM, et al (1999) An overview of the results of the
448 atmospheric model intercomparison project (amip i). Bulletin of the American
449 Meteorological Society 80(1):29–56
450 Gray WR, Wills RC, Rae JW, Burke A, Ivanovic RF, Roberts WH, Ferreira D,
451 Valdes PJ (2020) Wind-driven evolution of the north pacific subpolar gyre over
452 the last deglaciation. Geophysical Research Letters 47(6):e2019GL086,328
453 Grise KM, Davis SM (2020) Hadley cell expansion in cmip6 models. Atmospheric
454 Chemistry and Physics 20(9):5249–5268

455 Grise KM, Davis SM, Simpson IR, Waugh DW, Fu Q, Allen RJ, Rosenlof KH,
456 Ummenhofer CC, Karnauskas KB, Maycock AC, et al (2019) Recent tropical ex-
457 pansion: Natural variability or forced response? Journal of Climate 32(5):1551–
458 1571
459 Heffernan O (2016) The mystery of the expanding tropics. Nature News
460 530(7588):20
461 Hu Y, Fu Q (2007) Observed poleward expansion of the Hadley circulation since
462 1979. Atmospheric Chemistry and Physics 7(19):5229–5236
463 Kanamitsu M, Ebisuzaki W, Woollen J, Yang SK, Hnilo J, Fiorino M, Potter G
464 (2002) NCEP-DOE AMIP-II Reanalysis (r-2). Bulletin of the American Meteo-
465 rological Society 83(11):1631–1643
466 Kossin JP, Emanuel KA, Vecchi GA (2014) The poleward migration of the location
467 of tropical cyclone maximum intensity. Nature 509(7500):349
468 Lohmann G (2019) Temperatures from energy balance models: the effective heat
469 capacity matters. Earth System Dynamics Discussions pp 1–21
470 Lu J, Vecchi GA, Reichler T (2007) Expansion of the Hadley cell under global
471 warming. Geophysical Research Letters 34(6)
472 Medeiros B, Stevens B, Bony S (2015) Using aquaplanets to understand the robust
473 responses of comprehensive climate models to forcing. Climate Dynamics 44(7-
474 8):1957–1977
475 Min SK, Son SW (2013) Multimodel attribution of the southern hemisphere hadley
476 cell widening: Major role of ozone depletion. Journal of Geophysical Research:
477 Atmospheres 118(7):3007–3015
478 Norris JR, Allen RJ, Evan AT, Zelinka MD, ODell CW, Klein SA (2016) Evidence
479 for climate change in the satellite cloud record. Nature 536(7614):72–75
480 Polvani LM, Waugh DW, Correa GJ, Son SW (2011) Stratospheric ozone deple-
481 tion: The main driver of twentieth-century atmospheric circulation changes in
482 the Southern Hemisphere. Journal of Climate 24(3):795–812

Rackow T, Goessling HF, Jung T, Sidorenko D, Semmler T, Barbi D, Handorf D (2018) Towards multi-resolution global climate modeling with echam6-fesom. part ii: climate variability. Climate Dynamics 50(7):2369–2394

Ridgway KR (2007) Long-term trend and decadal variability of the southward penetration of the east australian current. Geophysical Research Letters 34(13)

Scheff J, Frierson D (2012) Twenty-first-century multimodel subtropical precipitation declines are mostly midlatitude shifts. Journal of Climate 25(12):4330–4347

Seidel DJ, Fu Q, Randel WJ, Reichler TJ (2008) Widening of the tropical belt in a changing climate. Nature geoscience 1(1):21–24

Shaw TA (2019) Mechanisms of future predicted changes in the zonal mean mid-latitude circulation. Current Climate Change Reports 5(4):345–357

Shaw TA, Tan Z (2018) Testing latitudinally dependent explanations of the circulation response to increased co2 using aquaplanet models. Geophysical Research Letters 45(18):9861–9869

Sidorenko D, Rackow T, Jung T, Semmler T, Barbi D, Danilov S, Dethloff K, Dorn W, Fieg K, Gößling HF, et al (2015) Towards multi-resolution global climate modeling with ECHAM6–FESOM. Part I: model formulation and mean climate. Climate Dynamics 44(3-4):757–780

Smith RS, Dubois C, Marotzke J (2006) Global climate and ocean circulation on an aquaplanet ocean–atmosphere general circulation model. Journal of climate 19(18):4719–4737

Son SW, Kim SY, Min SK (2018) Widening of the Hadley cell from Last Glacial Maximum to future climate. Journal of Climate 31(1):267–281

Staten PW, Rutz JJ, Reichler T, Lu J (2012) Breaking down the tropospheric circulation response by forcing. Climate dynamics 39(9-10):2361–2375

Staten PW, Reichler T, Lu J (2014) The transient circulation response to radiative forcings and sea surface warming. Journal of Climate 27(24):9323–9336

Staten PW, Lu J, Grise KM, Davis SM, Birner T (2018) Re-examining tropical expansion. Nature Climate Change 8:768–775

Stevens B, Giorgetta M, Esch M, Mauritsen T, Crueger T, Rast S, Salzmann M, Schmidt H, Bader J, Block K, et al (2013) Atmospheric component of the MPI-M Earth System Model: ECHAM6. Journal of Advances in Modeling Earth Systems 5(2):146–172

Stommel H (1948) The westward intensification of wind-driven ocean currents. Eos, Transactions American Geophysical Union 29(2):202–206

Thompson DW, Solomon S (2002) Interpretation of recent Southern Hemisphere climate change. Science 296(5569):895–899

Thompson DW, Solomon S, Kushner PJ, England MH, Grise KM, Karoly DJ (2011) Signatures of the Antarctic ozone hole in Southern Hemisphere surface climate change. Nature Geoscience 4(11):741

Wang Q, Danilov S, Sidorenko D, Timmermann R, Wekerle C, Wang X, Jung T, Schröter J (2014) The finite element sea ice-ocean model (fesom) v. 1.4: formulation of an ocean general circulation model. Geoscientific Model Development 7(2):663–693

Watt-Meyer O, Frierson DM (2019) Itcz width controls on hadley cell extent and eddy-driven jet position and their response to warming. Journal of Climate 32(4):1151–1166

Williams GP, Bryan K (2006) Ice age winds: An aquaplanet model. Journal of climate 19(9):1706–1715

Wu L, Cai W, Zhang L, Nakamura H, Timmermann A, Joyce T, McPhaden MJ, Alexander M, Qiu B, Visbeck M, et al (2012) Enhanced warming over the global subtropical western boundary currents. Nature Climate Change 2(3):161–166

Wu Y, Smith KL (2016) Response of northern hemisphere midlatitude circulation to arctic amplification in a simple atmospheric general circulation model. Journal of Climate 29(6):2041–2058

Yang H, Liu J, Lohmann G, Shi X, Hu Y, Chen X (2016a) Ocean-atmosphere dynamics changes associated with prominent ocean surface turbulent heat fluxes trends during 1958–2013. Ocean Dynamics 66(3):353–365

Yang H, Lohmann G, Wei W, Dima M, Ionita M, Liu J (2016b) Intensification and poleward shift of subtropical western boundary currents in a warming climate. Journal of Geophysical Research: Oceans 121(7):4928–4945

Yang H, Lohmann G, Krebs-Kanzow U, Ionita M, Shi X, Sidorenko D, Gong X, Chen X, Gowan EJ (2020a) Poleward shift of the major ocean gyres detected in a warming climate. Geophysical Research Letters DOI 10.1029/2019GL085868

Yang H, Lohmann G, Lu J, Gowan EJ, Shi X, Liu J, Wang Q (2020b) Tropical expansion driven by poleward advancing midlatitude meridional temperature gradients. Journal of Geophysical Research: Atmospheres 125(16):e2020JD033,158

Yin JH (2005) A consistent poleward shift of the storm tracks in simulations of 21st century climate. Geophysical Research Letters 32(18)

Zhou W, Xie SP, Yang D (2019) Enhanced equatorial warming causes deep-tropical contraction and subtropical monsoon shift. Nature Climate Change 9(11):834–839

Figures

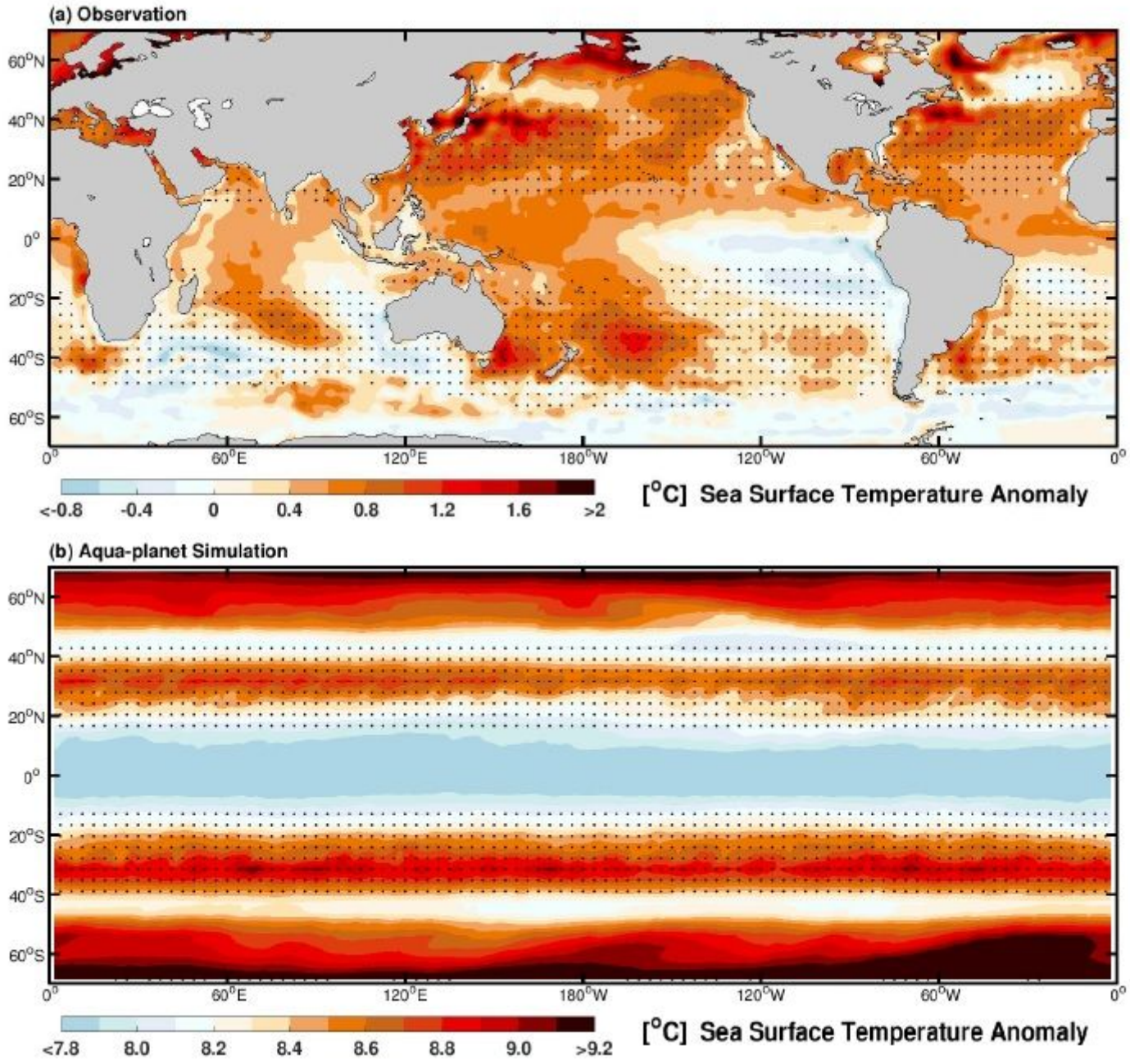

Figure 1

a: Observational Sea Surface Temperature (SST) anomaly during the most recent ve years of satellite period (2016-2020) with respect to the rst ve years (1982-1986). Relatively stronger ocean surface warming is found over all the subtropical oceans, likely due to the Ek- man convergence of background surface ocean currents. Result based on the NOAA Optimum Interpolation (OI) SST V2 dataset. The stippled area shows the subtropical convergence zone based on the near-surface wind stress curl elds from the NCEP-DOE reanalysis (1982-2020). b: Similar to A, but for SST anomaly in the last 40 years of the aqua-planet C1 global warming experiment with respect to the C0 control experiment. Unlike the

zonally symmetric enhanced subtropical ocean warming in the aqua-planet simulation, the observational enhanced subtropical ocean warming concentrates more towards the western ocean basins, where the centres of the subtropical gyres locate. Note: The designations employed and the presentation of the material on this map do not imply the expression of any opinion whatsoever on the part of Research Square concerning the legal status of any country, territory, city or area or of its authorities, or concerning the delimitation of its frontiers or boundaries. This map has been provided by the authors.

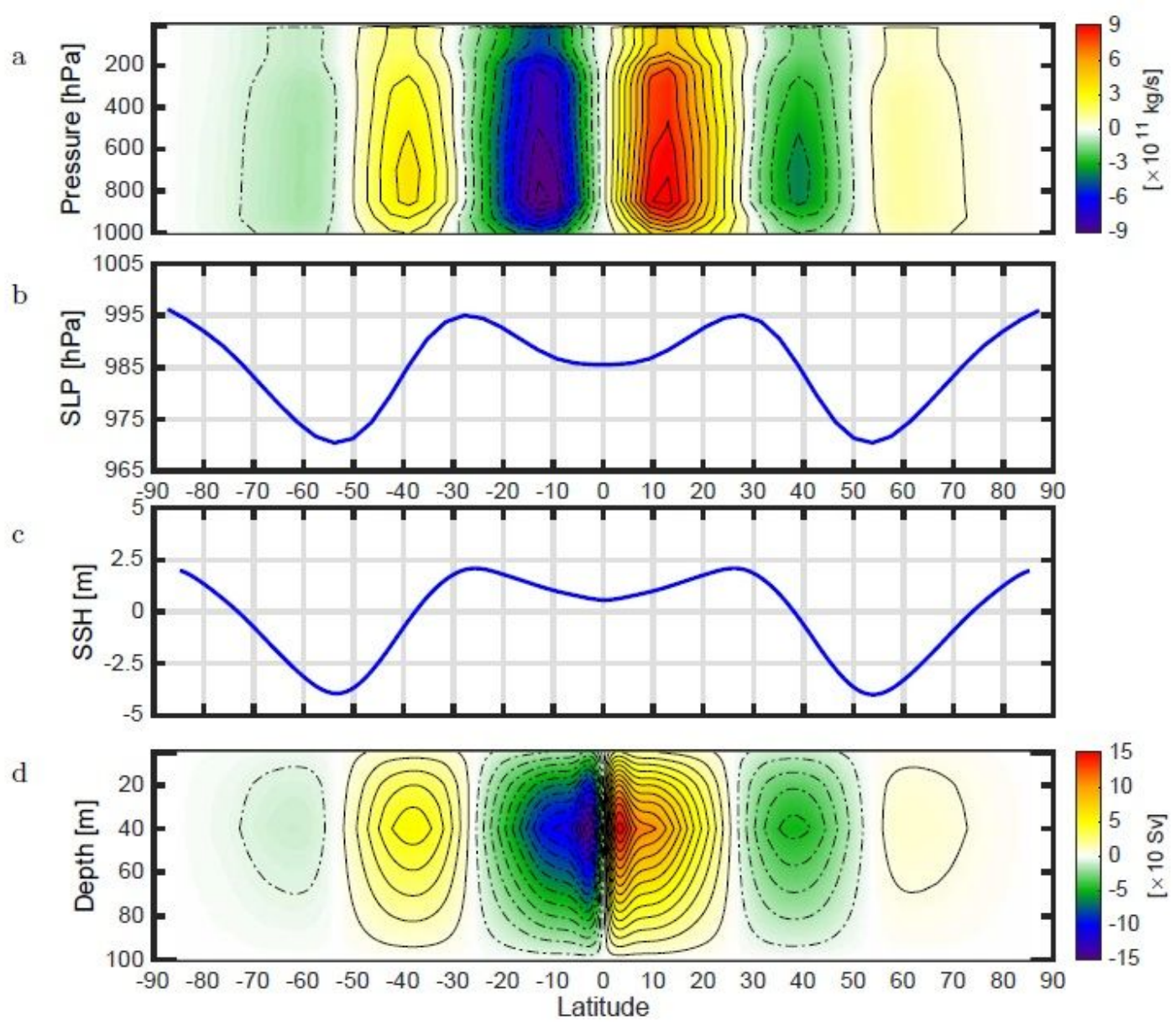

Figure 2

Climatological patterns of the atmosphere and ocean circulation in the aqua-planet C0 control experiment. a: Stream function of the atmospheric overturning circulation. Positive values represent clockwise ow, and negative values stand for anticlockwise ow. b: Sea level pressure (SLP). Subtropical high SLP is associated with sinking branches of the Hadley cell and the Ferrel cell, while subpolar low SLP is associated with the raising branches of the Ferrel cell and the Polar cell. c: Sea surface height

(SSH). Subtropical high SSH represents the centres of the real-world subtropical gyres, while subpolar low SSH denotes the position of the real-world subpolar gyre. d: Stream function of the overturning circulation in the ocean. Positive values represent clockwise ow, and negative values stand for anticlockwise flow.

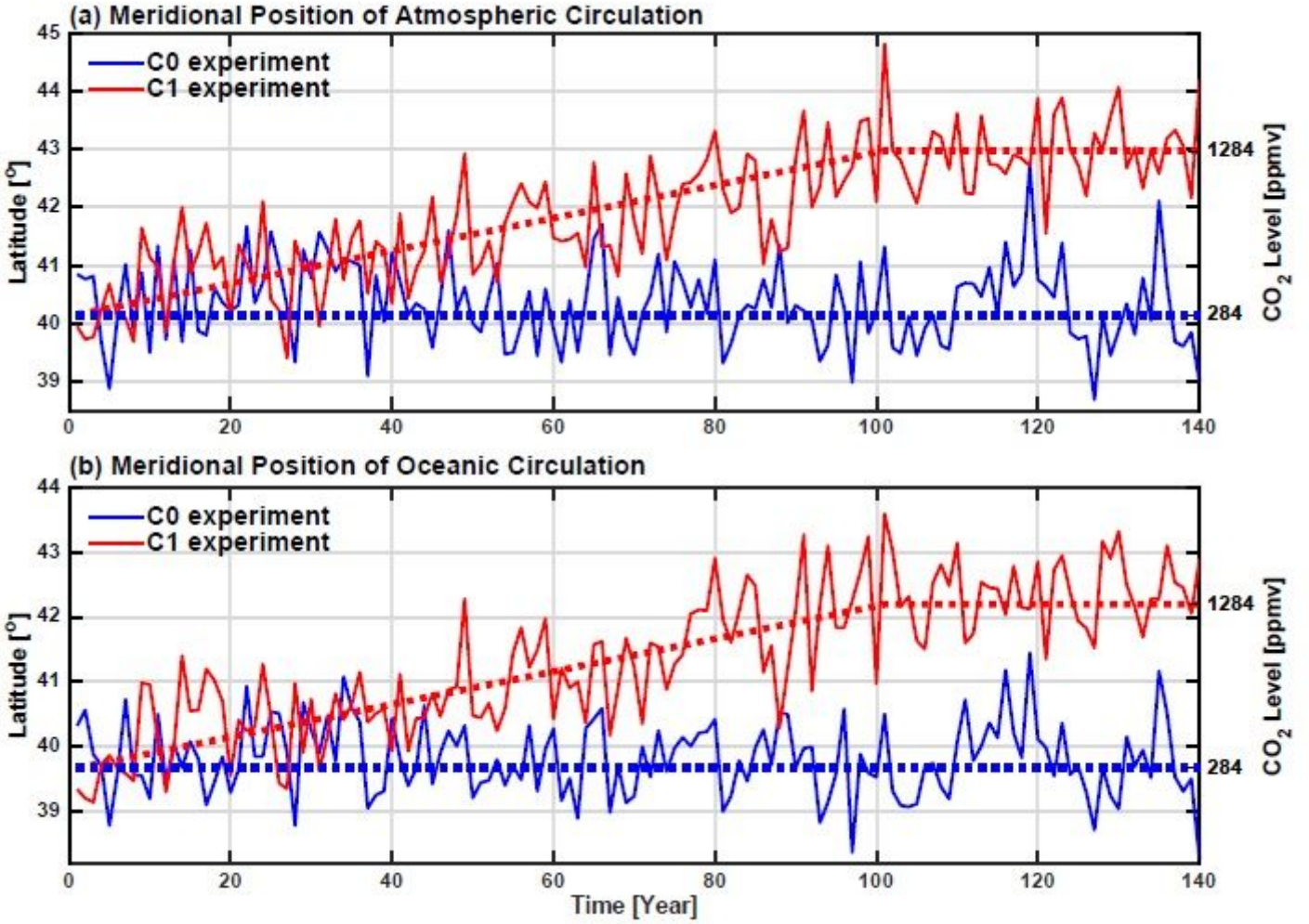

Figure 3

Meridional position of (a) atmospheric circulation and (b) oceanic circulation in the aqua-planet control (C0, blue lines) and global warming (C1, red lines) experiments. The solid lines represent the meridional position, and the dashed lines are the concentration of CO2. The displacement of the atmosphere circulation is strongly coupled with that of the ocean circulation. The correlation coefficients between them reach 0.82 and 0.95 in the C0 and C1 experiments, respectively.

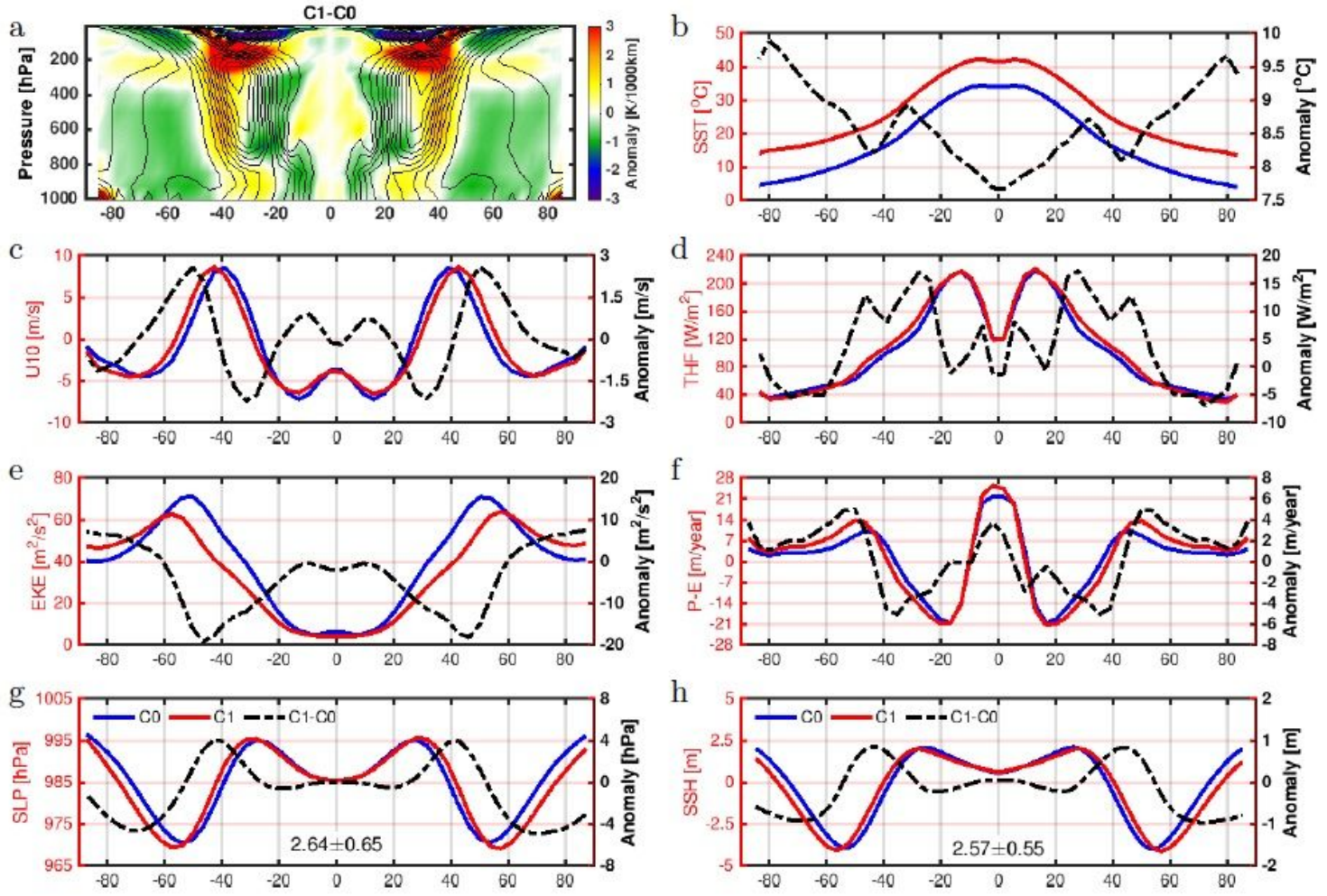

Figure 4

Comparison between aqua-planet C1 global warming experiment and C0 pre-industrial control experiment. (a). Meridional temperature gradient (MTG) anomaly (shading) in the C1 experiment with respect to the C0 control experiment. The contour lines provide the climatological pattern of the MTG in the C0 experiment. Zonal mean (b) sea surface temperature, (c) zonally near-surface wind, (d) ocean surface turbulent heat ux (THF, i.e., sensible + latent heat fluxes, positive-upward), (e) 850 hPa eddy kinetic energy (EKE) as indication of storm track, (f) precipitation minus evaporation (P-E), (g) sea level pressure (SLP), (h) sea surface height (SSH). The blue lines show the value of the control experiment (C0), the red lines show the values from the global warming experiment (C1), the dashed black lines are the difference between the global warming and the control experiments (C1-C0). The texts in the last two sub-panels provides the magnitudes of the poleward shift in the atmospheric and oceanic circulation, respectively. They are calculated based on the SLP and SSH fields, according to the definition introduced in section 2. All results are based on the last 40 years of the global warming experiment (C1) and 140 years of the control experiment (C0).

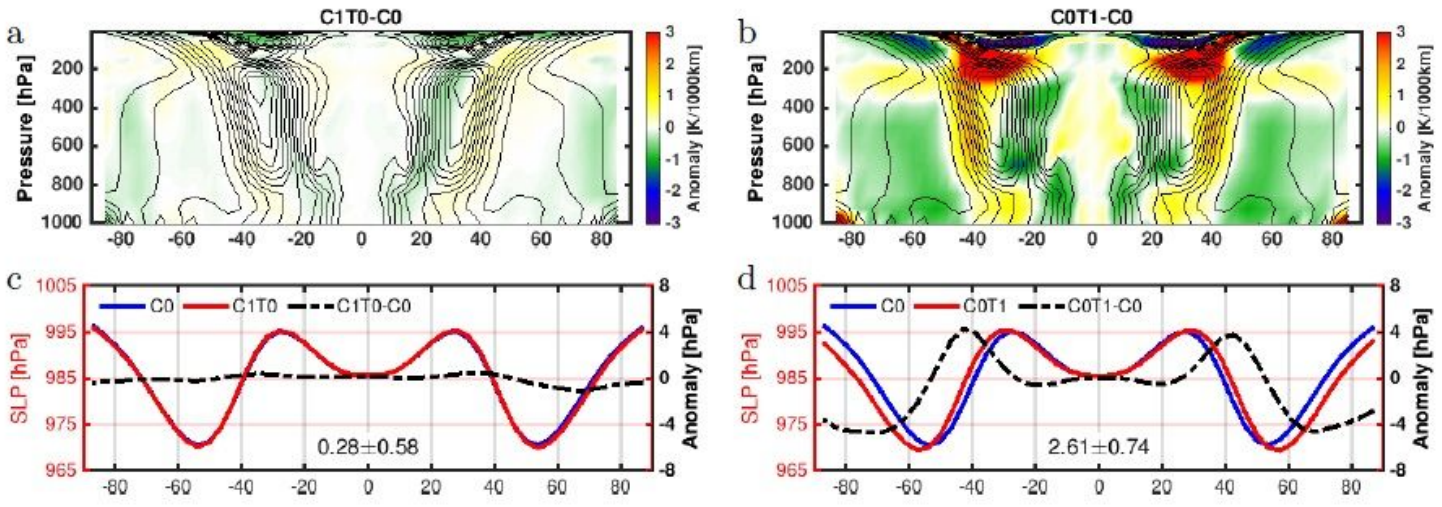

Figure 5

Similar to Fig. 4, but for comparison between aqua-planet C1T0 (left column, i.e., a and c), C0T1 (right column, i.e., b and d) experiments and the C0 pre-industrial control experiment. (a and b) Meridional temperature gradient (MTG) anomaly (shading). The contour lines provide the climatological pattern of the MTG in the C0 experiment. (c and d) Zonal mean SLP. The blue lines show the value of the control experiment (C0), the red lines show the values from the C1T0 and C0T1 experiment, the dashed black lines are the difference between the two experiments, i.e., C1T0-C0 and C0T1-C0. The poleward shifts in the C1T0 and C0T1 experiments are 0.28 and 2.61 degrees in latitude, respectively. Here, we only show the changes in SLP patterns to indicate the shift in the atmosphere circulation. It should be noted that the other metrics, like the P-E, winds, storm track, have consistent shift as well.

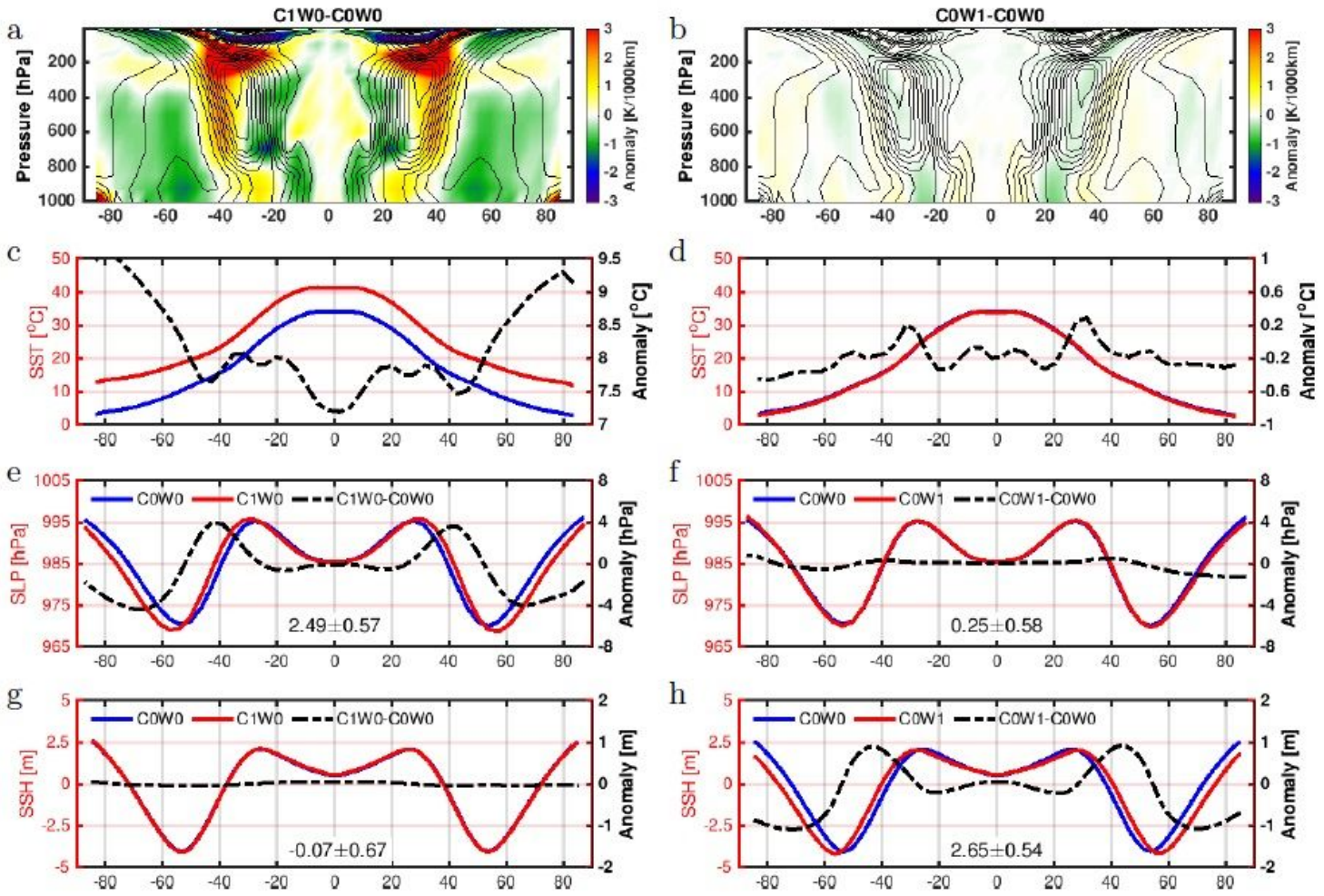

Figure 6

Similar to Fig. 4, but for results from the partially coupled C1W0 (a, c, e, g) and C0W1 (b, d, f, h) experiments with respect to the C0W0 control experiment.

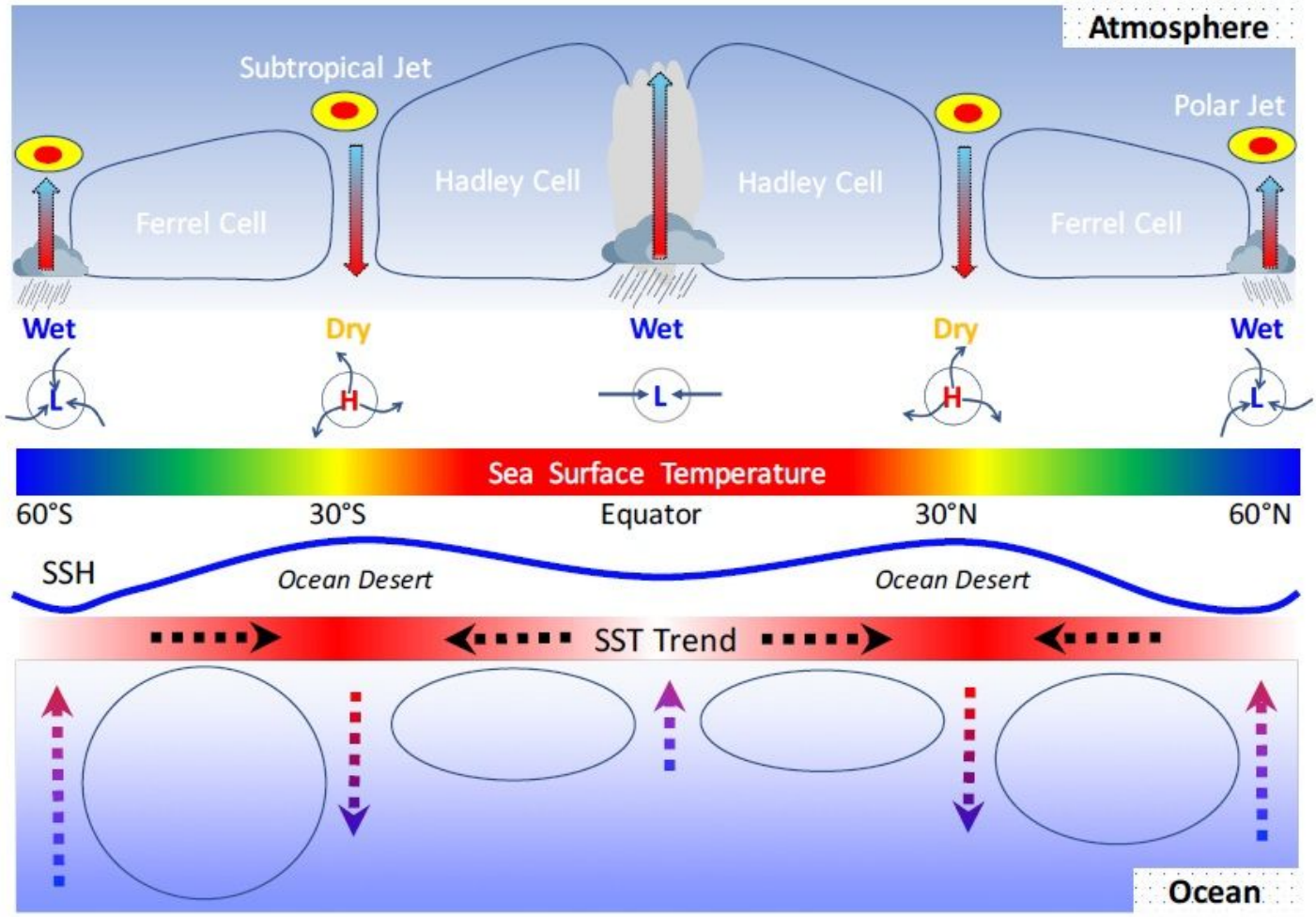

Figure 7

Schematic diagram showing how background ocean circulation promotes an enhanced subtropical ocean warming and drives the shift in the atmospheric and oceanic circulation. The arrows illustrate the significant features of atmosphere (solid) and ocean (dashed) circulation. From a climatological perspective, the maximum meridional temperature gradients (MTGs) locate at the subtropical to mid-latitude regions. Position of MTGs determines the position of the atmosphere circulation, thus the position of the wind-driven ocean circulation. Under the forcing of increasing greenhouse gases concentration, background Ekman convergence of surface currents favour an enhanced subtropical ocean warming. This enhanced warming expands the low latitude warm water zones, pushes the mid-latitude MTGs towards higher latitudes, thus forcing a poleward shift in the atmosphere circulation. The shift in the atmosphere circulation, associated with a corresponding shift in the near-surface wind then force a shift in the ocean circulation. Systematic shift of atmosphere and ocean circulation redistributes the natural resources, such as water, vegetation, marine primary productivity, hence has broad implications for our societies.

Supplementary Files

This is a list of supplementary files associated with this preprint. Click to download.

- Supplementarymaterial.docx